Nonlinear Behavior of the Reversed Field Pinch with Nonideal Boundary Conditions

Y. L. Ho[a] and S. C. Prager
Department of Physics, University of Wisconsin, Madison, Wisconsin 53706

D. D. Schnack
Science Application International Corporation, San Diego, California 92121
(Received 11 August 1988)

The effect of a resistive boundary and/or a distant conducting wall on a reversed field pinch is investigated with a three-dimensional magnetohydrodynamics code. Fluctuations rise with increasing distance between the conducting wall and the plasma. The enhanced fluctuation-induced $\mathbf{v}\times\mathbf{b}$ electric field primarily opposes toroidal current; hence loop voltage must increase to sustain the current. This increases the helicity injection rate, which is balanced by an enhanced surface loss.

PACS numbers: 52.65.+z, 52.35.Py, 52.55.Ez

Most reversed-field-pinch (RFP) theories and experiments have, until recently, included a highly conducting boundary near the plasma surface. Such a boundary condition is necessary for linear magnetohydrodynamic (MHD) stability,[1] for the minimum energy "Taylor state,"[2] and perhaps for the "dynamo sustainment"[3] of the RFP. Deviation from this ideal condition is useful to elucidate the essential physics ingredients of RFP sustainment, and may be of practical necessity. Long pulse experiments, such as the upcoming ZT-H[4] (as well as a controlled fusion reactor) will operate with a shell with a magnetic field penetration time much shorter than the plasma lifetime. This "thin shell problem" is now being experimentally studied in the OHTE,[5] HBTX-1C,[6] and Reversatron[7] devices. Of similar practical import is the determination of the required proximity of the conducting wall to the plasma surface (" the distant-wall problem"). Experiments in HBTX-1B[8] displayed anomalous increase in the toroidal loop voltage with insertion of limiters.

In this Letter, we computationally study the effect of a nonideal boundary on nonlinear resistive MHD dynamics. A 3D MHD code treats a plasma bounded by a thin resistive shell at minor radius $r=a$, which is itself surrounded by an outer perfectly conducting wall at $r=r_w>a$; a "vacuum" region of width r_w-a separates the resistive shell and conducting wall. The thin-shell problem and the distant-wall problem can both be studied by removing either the outer conductor or the resistive shell. Similar physics dominates each case. (The resistive shell presumably affects only the time evolution, not the final state.)

The code solves the full compressible MHD equations for a force-free, cylindrical plasma,[9] periodic in the z direction (with periodicity $2\pi R$). The resistivity varies radially as $\eta=\eta_0[1+9(r/a)^{30}]^2$, where η_0 is the characteristic plasma resistivity. Viscosity and mass density are spatially constant. The viscous term $\nu\nabla^2\mathbf{v}$ is included in the equation of motion principally for numerical stability; ν, the ratio of the viscous damping time to the resistive diffusion time τ_R $(=a^2\mu_0/\eta_0)$, is set at 2.5. The magnetic Lundquist number, S, is typically 6×10^3. The algorithm is finite differenced radially and pseudospectral in the other two dimensions. We employ 3 modes poloidally (poloidal mode number $m=0$ to 2), 43 modes axially (axial mode number $n=-21$ to 21), 127 points radially, and set $R/a=2.5$.

The boundary conditions at $r=a$ are as follows. The resistive shell, of thickness Δ and resistivity η_S, is modeled by a jump condition on the perturbed radial magnetic field b_r,[10]

$$\partial b_r/\partial t = a/\tau_S[\partial b_r/\partial r]\,, \tag{1}$$

where [ ] denotes a jump across the shell (assumed to be thin), and $\tau_S=\Delta a\mu_0/\eta_S$ is the shell penetration time. The mean $[(m,n)=(0,0)]$ velocity is given by $V_\theta=V_z=0$ and $V_r=|\mathbf{E}\times\mathbf{B}|/B^2$, where $\mathbf{E}$ and $\mathbf{B}$ are the mean electric and magnetic fields. The nonsymmetric velocity (m or n nonzero) vanishes at $r=a$, as appropriate for a viscous plasma. We assume that the radial current density also vanishes, as appropriate if the resistive wall is insulated from the plasma (which is often the case experimentally). Moreover, the magnetic shielding properties of the resistive shell can be shown to be independent of the radial current density at the boundary. The vacuum fields, between the resistive shell and conducting wall, are calculated analytically and matched to the plasma solution by Eq. (1). Linear benchmark computations agree with analytic (inviscid) linear calculation, except that highly localized modes, and modes resonant outside reversal, are damped in the computation. The discrepancy is due to differences in viscosity, edge resistivity, and velocity boundary condition. Initial equilibrium (mean field) profiles and fluctuation (nonsymmetric field) spectra are chosen to be that of an RFP plasma with a close-fitting perfectly conducting wall. This is generated by running the code with such a boundary condition until a dynamo-sustained quasi steady state is reached. The initial Θ is chosen to be 1.59, where $\Theta=B_\theta(a)/\langle B_z\rangle$ and $\langle\,\rangle$ denotes a volume

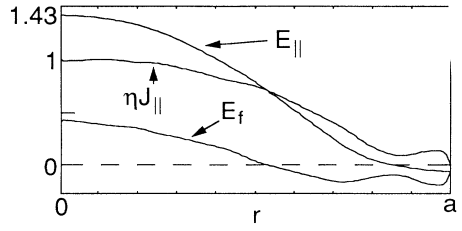

FIG. 1. Parallel electric field profiles for the steady-state close-fitting conducting wall case ($\Theta \sim 1.59$, $F \sim -0.08$). The electric fields are normalized to $\eta J_{||}$ at $r=0$. The total electric field, $E_{||}$, is composed of the Ohmic, $\eta J_{||}$, and the fluctuation induced E_f.

average.

Most of our results can be understood from the parallel component of the mean electric field $E_{||}$ ($=\mathbf{E}\cdot\mathbf{B}/|\mathbf{B}|$) and the fluctuation-induced electric field $E_f(=-\langle \mathbf{vb}\rangle_{\theta,z}\cdot\mathbf{B}/|\mathbf{B}|$, where $\langle\ \rangle_{\theta,z}$ denotes an average over θ and z). By Ohm's law, $E_{||}-E_f=\eta J_{||}$; thus, $E_{||}$ and E_f determine $J_{||}$, which in turn determines the stability and the level of dynamo activity present in a force-free RFP. The electric fields for the initial close-fitting conducting wall state are described here for later comparison with the nonideal boundary cases. Near a steady state, $\nabla\times\mathbf{E}\sim 0$ and $\mathbf{E}$ is just the applied toroidal electric field (constant with radius). From the radial profiles of the fields, Fig. 1, we see that the applied $E_{||}$ is of a shape to create a peaked λ profile, and by itself (without E_f) could not sustain a reversed field. (In steady state, $E_{||}$ in the reversed field region is $J_{||}$ suppressing, and hence E_f must be nonzero to satisfy Ohm's law.) Thus, from linear theory,[11] $E_{||}$ is destabilizing to the dynamo ($m=1$, $n<0$) modes. The E_f, generated primarily by the dynamo modes, however, is in a direction to flatten λ by current suppression near the center (positive part) and enhancement near the edge (negative part). This field generates reversal and a more stable profile (more shear). The mode saturation is a balance between this quasilinear stabilization (as well as nonlinear coupling to stable modes[12]) and the destabilization by the applied $E_{||}$.

If the conducting wall is removed (to a radius of $10a$) to treat the thin-shell problem, the fluctuating magnetic and kinetic energy increase by about 1 and 2 orders of magnitude, respectively. They appear to reach a plateau in about one shell time for $\tau_S=0.1\tau_R$, as shown in Fig. 2(a). The Θ value is held constant at 1.59. The n spectrum of $m=1$ fluctuations remains similar to the initial state, peaking at $n<0$ [Fig. 2(b)]. The loop voltage, Fig. 2(a), also increases with time, but develops giant excursions near the end of the computation (at $t\sim 1.2\tau_S$). This is not surprising in view of the parallel electric field profiles shown in Fig. 3. The E_f component is now about 7 times the resistive term ($\eta J_{||}$). Thus, modest variations in $\mathbf{v}$ or $\mathbf{b}$ can induce large current changes unless V_L adjusts accordingly. To balance the current suppression of

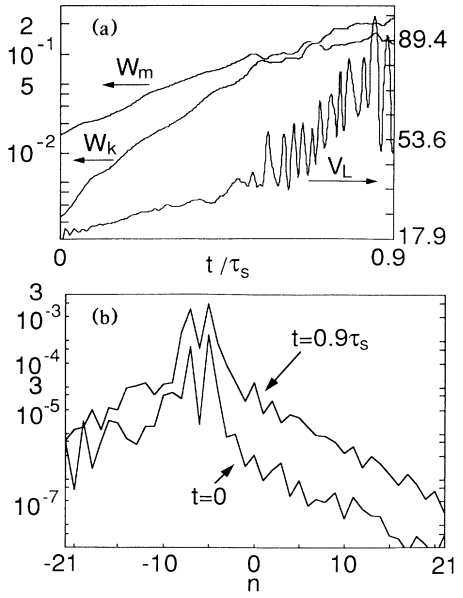

FIG. 2. Constant Θ evolution (initialized with a close-fitting conducting wall steady state) with a thin shell: (a) total radial magnetic energy [$W_m=\int 0.5(b_r/B_0)^2 d^3(r/a)$, where B_0 is the characteristic field strength], total kinetic energy (W_k, same units as W_m), and loop voltage [$V_L=(2\pi R/a)E_z(r=a)$, where E_z is normalized to $\eta J_{||}$ at $r=t=0$] vs time; (b) comparison of $m=1$ magnetic energy spectra at two different times.

E_f, V_L is now highly anomalous.

The dynamo modes, from quasilinear effects, are more strongly affected by the boundary than the linear theory implication (see Ref. 11 for the linear results). This is due to the enhanced E_f that primarily has $E_f>0$. The enhanced $E_{||}$ mainly balances the positive portion of E_f over most of the minor radius, leaving the $J_{||}$ profile relatively unchanged. The edge current drive of E_f deepens reversal, so that the reversal parameter F [$=B_z(a)/\langle B_z\rangle$] evolves from -0.08 to -0.15. The overall increase in shear due to the primarily positive E_f, however, is not

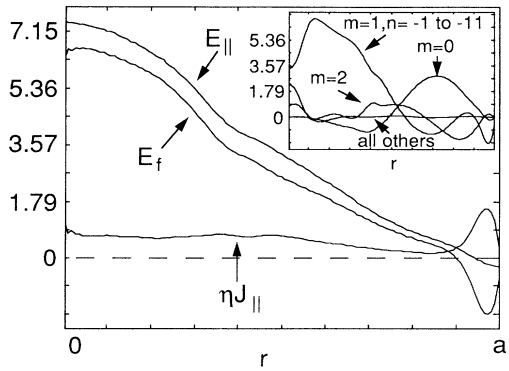

FIG. 3. Parallel electric field profiles at $t=0.9\tau_S$ for the constant Θ simulation with a thin shell, and (inset) the contributions to E_f from different bands.

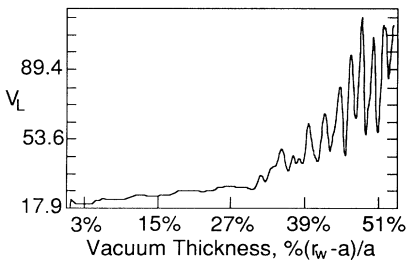

FIG. 4. V_L vs vacuum region thickness for the constant Θ and $\tau_S = 0.01\,\tau_R$ case.

sufficient to compensate for the loss of the conducting wall. Thus, the $m=1$, $n<0$ modes could not easily reestablish a new balance and saturate at a moderately increased amplitude. Hypothetically, if instability growth increases E_f only in the outer region where it drives $J_\parallel$, V_L would not be enhanced, and the growing $m=1, n<0$ modes can easily self-stabilize by the shear they generate (with sufficient shear, equilibria at $\Theta=1.59$ can be stable to $m=1, n<0$ modes even without a conducting wall). This idealized E_f profile may even lower V_L, since $J_\parallel$ in the outer region contains a positive toroidal component as well.

To distinguish the effects of various modes, in Fig. 3 (inset) we plot the contribution to E_f of different spectral bands. The $m=0$ contribution is mainly in a direction to suppress $J_\parallel$ in the periphery; thus, $m=0$ modes (which also grow to large amplitude) are quasilinearly destabilizing to $m=1$ modes. However, the overall effect of $m=0$ modes is stabilizing; removal of $m=0$ modes yields a twentyfold increase in V_L. Thus, nonlinear mode coupling is probably the dominant stabilizing influence. The n spectrum of the $m=1$ modes is broadened by the $m=0$ presence. The broadened spectrum more efficiently cascades energy to small scale, stable, dissipative modes.[12] Contributions to E_f from modes other then the dynamo and $m=0$ modes are weak.

We generally do not observe large $m=1$, $n>0$ external kinks, as we expected from linear theory. However, preliminary runs at higher Θ and deeper reversal indicate larger $n>0$ kinks. Single helicity runs show that these modes also suppress $J_\parallel$.[13]

When the conducting wall is placed closer to the plasma boundary to treat the distant-wall problem, the fluctuations and V_L saturate at lower amplitude in the constant Θ simulations. To track the dependence of V_L on the wall position, r_w, we expand the wall slowly during one run. The total electric field is nearly curl-free during the simulation; thus the plasma maintains a quasi steady state. Individual modal behavior for the dominant modes is also relatively quiescent, i.e., $\partial/\partial t \sim 0$. Hence, the boundary condition, Eq. (1), is independent of τ_S, and this case is relevant to the experimental situation of a plasma separated from the wall by limiters. From Fig. 4 ($\tau_S=0.01$ for the case shown, but the $\tau_S=0.002$ and 0.1 cases behave similarly), we see that V_L rises with r_w, increasing dramatically beyond $r_w \sim 1.33a$, at which point oscillations in V_L begin. At higher Θ values the rise in V_L is more dramatic. At $\Theta=1.73$, V_L rises by 50% as r_w increases from a to $1.05a$.

It is instructive to interpret our results in terms of conservation of magnetic helicity.[2] The requirement of helicity balance in steady state has been used to model anomalous V_L in experiments with limiter insertion.[14,15] Here, we evaluate quantitatively the terms in the helicity balance equation. We thereby identify the enhanced helicity loss channel associated with the V_L increase.

Generally, helicity balance in steady state requires the injected helicity ($V_L\Phi_z$) to balance the plasma dissipation ($\int \eta \mathbf{J}\cdot\mathbf{B}\,d^3r + \int \eta \mathbf{j}\cdot\mathbf{b}\,d^3r$), and surface losses[15] ($-\int_S \chi \mathbf{b}\cdot d\mathbf{s}$, where χ is the electrostatic surface potential), i.e.,

$$V_L\Phi_z = \int \eta \mathbf{J}\cdot\mathbf{B}\,d^3r + \int \eta \mathbf{j}\cdot\mathbf{b}\,d^3r - \int_S \chi \mathbf{b}\cdot d\mathbf{s}. \quad (2)$$

In our model, the surface potential is caused by obstruction of current flow by the resistive shell which is penetrated by the perturbed magnetic flux. Surface charges accumulate (producing the surface potential) to keep $j_r=0$ on the plasma surface while maintaining continuity of e_θ and e_z. Using Eq. (2), Jarboe and Alper proposed that if the insertion of limiters lead to an increase in helicity dissipation in the plasma (particularly in the edge region), V_L must rise to maintain helicity balance.[14] In addition, Tsui proposed that enhanced surface helicity loss, which he calculated from kinetic sheath effects for an inserted limiter, also implies an enhanced V_L.[15] Our evaluation of the terms appearing in Eq. (2)

TABLE I. Evaluation of the terms appearing in the helicity balance equation [Eq. (2)] for different distant wall cases in dimensionless units (for relative comparison only).

Θ, % vacuum	$V_L\Phi_z$	$\int \eta \mathbf{J}\cdot\mathbf{B}\,d^3r$	$\int \eta \mathbf{j}\cdot\mathbf{b}\,d^3r$	$-\int_S \chi \mathbf{b}\cdot d\mathbf{s}$
1.592, 0%	24.5	24.9	0.5	0
1.592, 15%	32.9	25.1	1.4	6.2
1.592, 45%	43.6	25.5	2.6	13.1
1.73, 0%	32.7	33.7	0.8	0
1.73, 5%	48.2	37	2.7	6.2

for various distant-wall cases are listed in Table I, which shows that the resistive helicity dissipation in the plasma increases negligibly with enhanced fluctuations (comparing cases with the same Θ but different vacuum region width). In addition, the edge region does not dissipate helicity at a disproportionate level compared with the bulk flasma (not shown). The increased helicity input is lost through the surface term, as suggested by Tsui. With our model, however, we obtain a self-consistent treatment, which includes E_f as the mechanism causing the rise in V_L. The vacuum region is destabilizing, and current flow is interrupted when the perturbed magnetic field enters a vacuum region, leading to surface helicity loss. Thus, vacuum-induced instability implies surface helicity leakage and vice versa. The instability both enhances the helicity input by raising V_L (through E_f), and enhances the surface helicity leakage.

In conclusion, the conducting wall is a key element in the MHD dynamics of the RFP. It is well known that with a close-fitting conducting wall the internally resonant $m=1$ modes, through their $\mathbf{v}\times\mathbf{b}$ effect, drive current in the edge to sustain reversal; also, when combined with current suppression at the center, the effect is to flatten the $\lambda(=j/B)$ profile, which allows the modes to self-stabilize. This fluctuation-induced electric field, along with nonlinear stabilization via mode coupling, is balanced by the applied electric field which has the destabilizing effect of peaking λ. Removal of the wall disturbs this balance; the $m=1$ modes grow, suppress the central current, and thereby require an enhanced loop voltage to maintain the current. The increase in the $\mathbf{v}\times\mathbf{b}$ electric field, combined with the rising V_L, produces little increase in shear for self-stabilization of the $m=1$ modes. Thus, $m=1$ modes and V_L grow to a large amplitude. The enhanced helicity input is lost through the surface from fluctuation-induced surface potentials. These effects occur with either a resistive or distant boundary. The anomalous loop voltage present in some RFP experiments with limiter insertion may result from such MHD effects. Interestingly, the conducting wall serves the useful purpose of preventing the dynamo modes from becoming too robust.

The utility of this MHD computation is to depict key physical mechanisms that influence the plasma as the boundary is varied. A comprehensive picture, even within MHD, will require inclusion of other important effects, such as equilibrium rotation, plasma pressure, higher-S values, different pinch parameters, etc. MHD computation can also examine the possibility of alternative stabilization schemes, such as feedback stabilization through electrical means at the boundary.

This work was supported by the U.S. DOE.

---

[a]Current address: Science Application International Corporation, San Diego, CA 92121.

[1]D. C. Robinson, Nucl. Fusion **18**, 939 (1978).

[2]J. B. Taylor, Rev. Mod. Phys. **58**, 741 (1986).

[3]See, for example, E. J. Caramana and D. D. Schnack, Phys. Fluids **29**, 3023 (1986); A. Y. Aydemir and D. C. Barnes, Phys. Rev. Lett. **52**, 930 (1984); H. R. Strauss, Phys. Fluids **27**, 2580 (1984).

[4]P. Thullen, Bull. Am. Phys. Soc. **31**, 1546 (1986).

[5]T. Tamano, W. D. Bard, C. Chu, Y. Kondoh, R. J. La Haye, P. S. Lee, M. T. Saito, M. J. Schaffer, and P. L. Taylor, Phys. Rev. Lett. **59**, 1444 (1987).

[6]B. Alper, in *Proceedings of the IEEE International Conference on Plasma Science, Seattle, Washington, 1988* (IEEE, New York, 1988), paper No. 5P17.

[7]S. Robertson and P. Schmid, Phys. Fluids **30**, 884 (1987).

[8]B. Alper and H. Y. W. Tsui, in *Proceedings of the Fourteenth European Conference on Controlled Fusion and Plasma Physics, Madrid, Spain, June 1987,* edited by S. Methfessel (European Physical Society, Budapest, 1987), Vol. 2, p. 434.

[9]D. D. Schnack, D. C. Barnes, Z. Mikic, D. S. Harned, and E. J. Caramana, J. Comput. Phys. **70**, 330 (1987).

[10]C. G. Gimblett, Nucl. Fusion **26**, 617 (1986).

[11]Y. L. Ho and S. C. Prager, Phys. Fluids **31**, 1673 (1988).

[12]J. A. Holmes, B. A. Carreras, P. H. Diamond, and V. E. Lynch, Phys. Fluids **31**, 1166 (1988).

[13]Y. L. Ho, S. C. Prager, and D. D. Schnack, Bull. Am. Phys. Soc. **32**, 1832 (1987).

[14]T. R. Jarboe and B. Alper, Phys. Fluids **30**, 1177 (1987).

[15]H. Y. W. Tsui, Culham Laboratory Report No. CLM-P819 (to be published).